Supplementary Material (ESI) for Lab on a Chip

Supporting Information

1. Operating principle and governing equations

Single-walled carbon nanotubes (SWCNTs) transistors operate through modulation of Schottky barrier height [1] as a result from applied gate bias (V_G) at the proximity of a semiconducting channel. In this perspective, a semiconducting nanotube which is brought into contact with metallic source/drain electrode pad would result in pinning of the Fermi level at the semiconductor/metal junction. Hence, when the work function of the metals is different from that of the nanotubes, the valence and conduction band of the later bends accordingly to conform to the pining at the junction. Such band bending, hence, leads to generation of a Schottky barrier whose height and width determines the conductivity of the overall architecture. In brief, the transistor characteristics hence is originated from modulation of this Schottky barrier as a result from non-contact influence of a third voltage V_G at the proximity of the nanotubes.

Mathematically, the modulation of the Schottky barrier can be represented in Landauer-Buttiker formula [2-4], as shown below:

Equation 1

$$I_{DS}(V_G) = \frac{4q^2}{h} \sum_i \int_{E_1}^{E_2} T_n(E, V_G)\left(f_S(E) - f_D(E, V_{DS})\right) dE$$

In this formula, the q and h denote the elemental charge and Planck's constant, respectively while the T_n, f_S, and f_D refer to the effective transmission probability and Fermi-Dirac probability at source and drain junction, respectively.

The summation in Equation 1 is performed throughout the conducting channels in the nanotubes, and the integration was carried out from the smallest energy level in the conduction band to the first Brillouin-zone of the energy-momentum diagram of the nanotube. The $T_n\ (E,V_G)$ in Equation 1 is governed by Wentzel-Kramers-Brillouin (WKB) approximation (Equation 2) which has been shown appropriate to treat stepwise discontinuous potential such as one found at the metal/semiconductor junction in the liquid-gated field-effect transistor (LGFET) architecture [3]. At the individual source and drain junction, the transmission probability is governed by the following equation:

Equation 2

$$T_{nS/D}(E,V_G) = \exp\left(-\int_{z_i}^{z_f} \frac{2E_g}{3dV_{pp\pi}} \sqrt{\left(\frac{3dV_{pp\pi}k_n}{E_g}\right)^2 - \left(\frac{E - E_{S/D}(z)}{E_g/2}\right)} dz \right)$$

In Equation 2, the z_i, z_f, E_g, d, $V_{pp\pi}$, k_n , and $E_{S/D}$ denote the initial junction point, the end-point of the band-bending, the band-gap, the carbon-carbon bond distance (0.142 nm) [3], nearest-neighbor interaction energy (2.97 eV, conducting channel wavenumber, and the energy band profile in the nanotubes respectively.

As it can be appreciated from Equation 2, the T_n is influenced not merely by the V_G, but

also a number of other factors some of which are innate electrical properties from the nanotubes themselves, such as the E_g, the k_n, and the $V_{pp\pi}$. The integration in Equation 2 is performed from the initiation point of the band bending up to the Schottky barrier width regime when the energy profile ceases to bend, which is commonly defined as the region when the gradient of the band $dE_{S/D}/dz$ goes to zero.

Hence, the energy profile at the nanotube/metal junction should be obtained and solved as a pre-requisite to solving Equation 2. To obtain the expression of the band profile at the junction, Jimnez et al [3] solved the Laplace equation (Equation 3) which governs electrostatic potential distribution in an enclosed boundary utilizing cylindrical coordinate as a proxy to the geometry of the nanotubes:

Equation 3

$$\frac{1}{r}\frac{\partial}{\partial r}\left(r\frac{\partial E(r,z)}{\partial r}\right)+\frac{\partial^2 E(r,z)}{\partial z^2}=0$$

Equation 4

$$E(r=0,z=0)=\varphi_{SB} \qquad E(r=0,z=\infty)=\varphi_{SB}-e(V_G-V_T)$$

By applying the boundary conditions as stated in Equation 4 to Equation 3, the $E_{S/D}$ profile can be obtained, and assume a general form of Equation 5 and 6 for source and drain junction, respectively.

Equation 5

$$E_S = \varphi_{SB} - e(V_G - V_T)\left(1 - \exp\left(-\frac{2z}{t_{dielectric}}\right)\right)$$

Equation 6

$$E_D = (\varphi_{SB} - eV_{DS}) - e(V_G - V_T)\left(1 - \exp\left(-\frac{2(z-L)}{t_{dielectric}}\right)\right)$$

The φ_{SB}, V_{DS}, L, and $t_{dielectric}$ in Equation 5 and 6 denote the Schottky barrier height, the source-drain bias, the length of the nanotubes, and thickness of the dielectric layer in the nanotube transistor, which influence the total capacitance in the transistor architecture. The V_T appears in both equations is to represent the threshold potential, which is governed by the classical relationship shown in Equation 7, whereby the Q_i and $C_{quantum}$ are to denote the charge contributed from the biomolecules, and the quantum capacitance of the nanotubes (4×10^{-19} F nm^{-2}) [5], respectively.

Equation 7

$$V_T = \sum_i \frac{Q_i}{C_{total}}$$

An applied V_{DS} across the metal/semiconductor/metal architecture commonly found in the Schottky transistor results in flowing of charge carriers from high to low energy state, whose direction is dependent on whether the predominant carrier is that of holes, or

electrons. Upon traveling from source to drain electrodes, the carriers encounter two Schottky barriers at the source and drain junctions, both of which influence the conductivity of the nanotubes. Hence, to simplify the calculation in Equation 1, the effective T_n is is affected by both T_{nS} and T_{nD}, as governed in Equation 8

Equation 8

$$T_n = \frac{T_{nS} T_{nD}}{T_{nS} + T_{nD} - T_{nS} T_{nD}}$$

Equations 5 to 8 enable us to account for contributions from Schottky barriers, electrostatic-gating, and capacitance on $T_{nS/D}$ (Equation 2), further leading to their effect on I_{DS} (Equation 1).

2. Electrical conductance of SWCNTs in non-ballistic regime

In the typical experimental condition that we encounter, the nanotubes are not operated in the ballistic regime, which indicates that the diffusive transport mode plays a role in the conduction of the electrical charge in the SWCNTs and the mobility is not infinite. Hence, to take into account diffusive transport in the I_{DS} model, Heller et al [4] cascaded the conductance as derived from the I_{DS} found from the Landauer-Buttiker formula (Equation 1) in series (Figure 1) with another conductance which is governed by classical Drude's formula (Equation 9) whereby n and μ represent charge carrier concentrations and mobility. The resultant conductance is then calculated from the traditional electric

circuit theory as stated in Equation 10, and the effective I_{DS} is calculated based on the Equation 9 through multiplication with the corresponding V_{DS}.

Equation 9

$$G = \frac{1}{en\mu}$$

Equation 10

$$\frac{1}{G_{resul\tan t}} = \frac{1}{G_{Drude}} + \frac{1}{G_{Landauer-Butti\ker}}$$

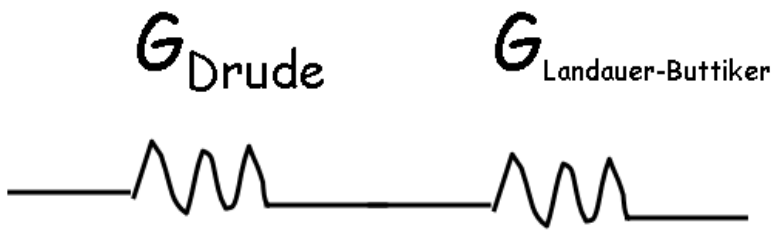

Figure S1 Conductance as obtained from Landauer-Buttiker formula cascaded in series with another conductance as derived from Drude formula to take into account the effect of diffusive transport in the resultant I_{DS}.

3. Possible sensing mechanisms in SWCNT LGFET biosensors

From the above equations, it can be appreciated that there are four possible sensing mechanisms [4] which reflect the interaction between biomolecules and LGFETs: (1)

electrostatic gating, (2) Schottky barrier modulation, (3) capacitance, and (4) mobility change; each of which displays a unique characteristic change in the I_{DS}-V_G curve (Figure 2 (a) – (d)). Electrostatic gating is associated with a shift in I_{DS}-V_G curve (positive or negative), depending on the charge of the biomolecules binding to the nanotubes. Modulation of the Schottky barrier is characterized by a decrease in I_{DS} at negative V_G bias, and increase in I_{DS} at positive V_G bias. A change in the capacitance is typified by modulation in the saturation current, whereas mobility changes caused by scattering or other effects of biomolecule/SWCNT interaction show a decrease in gradient under both positive and negative V_G bias.

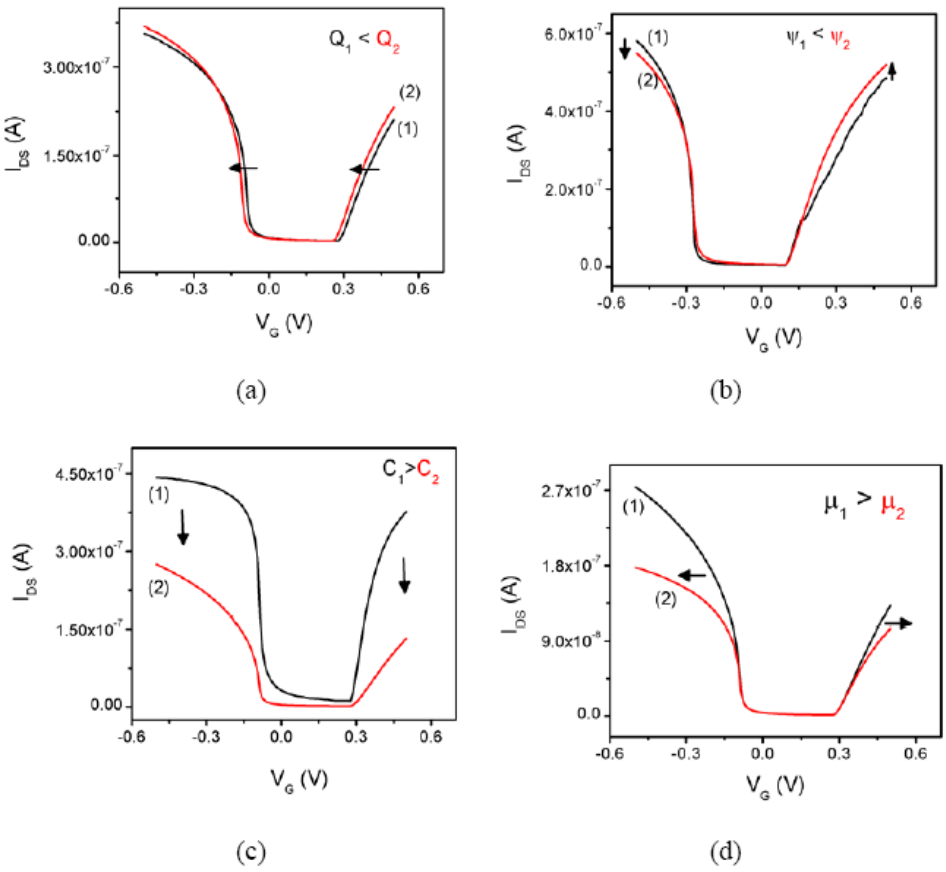

Figure S2 Four possible sensing mechanisms [4] which reflect the interaction between a biomolecule and nanotubes. As noted, each mechanism displays a unique characteristic change in the I_{DS}-V_G curve, which can be utilized to determine the predominant interaction between biomolecules and nanotubes.

In the calculation reported herein, we have employed the following parameters as baseline: φ_{SB} 0.5 eV [2], $C_{quantum}$ 4 x 10^{-19} F nm^{-2} [5], $C_{dielectric}$ 6.9 x 10^{-19} F nm^{-2} [6] which corresponds to the Debye capacitance for the buffer solution used in the experimentation,

μ 800 $cm^2V^{-1}s^{-1}$, and Q_i 0 Coulomb. Note that the mobility found from simulation is much lower than typically reported in the literature [7], revealing the non-trivial contribution from the diffusive transport in our LGFET owing to the fact that the device constitutes a random network of nanotubes causing large reduction in mobility. Furthermore, two parameters are modified upon adsorption of Poly (L-Lysine) (PLL) which correspond to electrostatic gating and capacitance change as observed from the experimental I_{DS}-V_G curve. In particular, the Q_i, ε_r and $C_{dielectric}$ are changed to 8 x 10^{-19} Coulombs, 10, and 4.033 x 10^{-19} F nm^{-2} in that order, and the latest of which corresponds to the typical capacitance for biomolecules. Additionally, to express the individual contribution from the two mechanisms, three simulations are performed: exclusive contribution from (1) electrostatic gating, or (2) capacitance, and combined involvement of (3) electrostatic-gating and capacitance.

4. The influence of applied frequency and V_G bias on the kinetic measurement

The pulsed-gating approach is introduced to avoid the electrolysis of water, so that the LGFET can be operated across a large operating voltage range. Pulsed-gating avoids the electrolysis through kinetic prevention of the water splitting reaction. In specific, the applied bias in pulsed-gating lasts for only a fraction of a millisecond: too fast for the electrolysis reaction to takes place.

Application of pulsed-gating in and all by itself does not modify the performance of the LGFET, as shown from the comparison between the I_{DS} and the leakage current (I_{leak})

(Figure 1(d) in the manuscript). It is also important to determine the influence of applied frequency and V_G bias on the kinetic measurement.

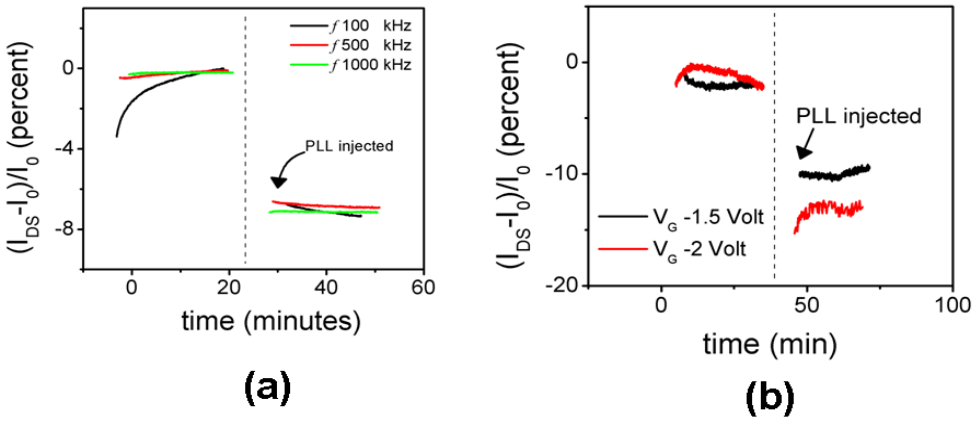

Figure S3 (a) frequency response of the I_{DS} at 100 kHz, 500 kHz, and 1000 kHz before and after exposure toward PLL. Overlaps in the response indicate that the I_{DS} is independent of applied frequency of pulsed-gating. (b) The magnitude of the signal depends on the applied V_G. Larger signal is obtained at higher $|V_G|$ range.

The absence of appreciable change in I_{DS} as a function of frequency (Figure S3 (a) indicates that the I_{DS} is independent of the applied frequency in tested window of 100 kHz to 1 MHz. The magnitude of the I_{DS} change, however, is influenced by the applied pulsed $|V_G|$ chosen as shown in Figure 3 (b). Larger applied $|V_G|$ results in larger signal level and would improve the detection limit.

References

[1] A. Javey, J. Guo, Q. Wang, M. Lundstrom, and H. Dai, Nature **424** (6949), 654 (2003).

[2] H. Arash, K. Tejas, and H. S. P. Wong, Electron Devices, IEEE Transactions on **54** (3), 439 (2007).

[3] D. Jimnez, X. Cartoix, E. Miranda, J. Su, F. A. Chaves, and S. Roche, Nanotechnology **18** (2), 025201 (2007).

[4] I. Heller, A. M. Janssens, J. Mannik, E. D. Minot, S. G. Lemay, and C. Dekker, Nano Letters **8** (2), 591 (2008).

[5] S. Ilani, L. A. K. Donev, M. Kindermann, and P. L. McEuen, Nature Physics **2** (10), 687 (2006).

[6] K. Maehashi, T. Katsura, K. Kerman, Y. Takamura, K. Matsumoto, and E. Tamiya, Analytical Chemistry **79** (2), 782 (2006).

[7] T. Durkop, S. A. Getty, E. Cobas, and M. S. Fuhrer, Nano Letters **4** (1), 35 (2003).

Supplementary Material (ESI) for Lab on a Chip